

Design, Synthesis, and Structure–Activity Relationship Studies of Fluorescent Inhibitors of Cyclooxygenase-2 as Targeted Optical Imaging Agents

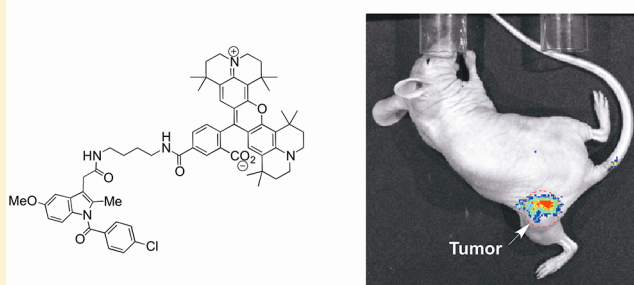
Md. Jashim Uddin, Brenda C. Crews, Kebreab Ghebreselasie, and Lawrence J. Marnett*

A. B. Hancock, Jr., Memorial Laboratory for Cancer Research, Department of Biochemistry, Chemistry and Pharmacology, Vanderbilt Institute of Chemical Biology, Center for Molecular Toxicology and Vanderbilt-Ingram Cancer Center, Vanderbilt University School of Medicine, Nashville, Tennessee 37232-0146, United States

S Supporting Information

ABSTRACT: Cyclooxygenase-2 (COX-2) is an attractive target for molecular imaging because it is an inducible enzyme that is expressed in response to inflammatory and proliferative stimuli. Recently, we reported that conjugation of indomethacin with carboxy-X-rhodamine dyes results in the formation of effective, targeted, optical imaging agents able to detect COX-2 in inflammatory tissues and premalignant and malignant tumors (Uddin et al. *Cancer Res.* **2010**, *70*, 3618–3627). The present paper summarizes the details of the structure–activity relationship (SAR) studies performed for lead optimization of these dyes. A wide range of fluorescent conjugates were designed and synthesized, and each of them was tested for the ability to selectively inhibit COX-2 as the purified protein and in human cancer cells. The SAR study revealed that indomethacin conjugates are the best COX-2-targeted agents compared to the other carboxylic acid-containing nonsteroidal anti-inflammatory drugs (NSAIDs) or COX-2-selective inhibitors (COXIBs). An *n*-butyldiamide linker is optimal for tethering bulky fluorescent functionalities onto the NSAID or COXIB cores. The activity of conjugates also depends on the size, shape, and electronic properties of the organic fluorophores. These reagents are taken up by COX-2-expressing cells in culture, and the uptake is blocked by pretreatment with a COX inhibitor. In *in vivo* settings, these reagents become highly enriched in COX-2-expressing tumors compared to surrounding normal tissue, and they accumulate selectively in COX-2-expressing tumors as compared with COX-2-negative tumors grown in mice. Thus, COX-2-targeted fluorescent inhibitors are useful for preclinical and clinical detection of lesions containing elevated levels of COX-2.

COX-2-Targeted Imaging Agents



■ INTRODUCTION

Early detection is one of the critical challenges for contemporary clinical cancer care. Detection of small premalignant lesions and early stage primary tumors is crucial for effective cancer therapy. For this reason, interest in highly sensitive imaging techniques for clinical oncology has increased tremendously in recent decades. Many groups have studied the *in vivo* detection of tumors using contrast agents appropriate for various imaging modalities.^{1–3} Methods have been developed for specific targeting in order to maximize the localization of ligands in the tumor and to minimize the uptake in the surrounding normal tissues to achieve high signal-to-noise ratios.^{4–6} These approaches include targeted imaging of tumors using monoclonal antibodies that specifically bind to receptors on the tumor cells,^{7,8} protease-activated near-infrared fluorescent probes for detection of tumors,⁹ folate receptor-targeted *in vivo* imaging of tumors using a near-infrared (NIR) dye-folate conjugate,¹⁰ and integrin-targeted imaging of lung and liver metastases using a ⁶⁴Cu-1,4,7,10-tetraazacyclododecane-1,4,7,10-tetraacetic acid (DOTA) dimeric arginylglycylaspartic acid peptide radiotracer.¹¹

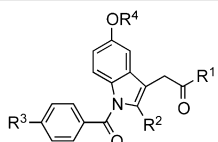
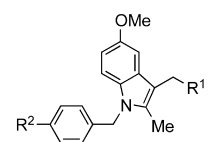
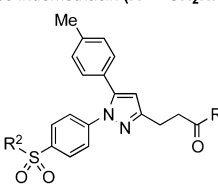
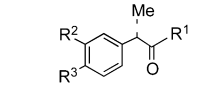
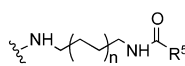
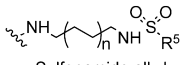
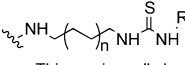
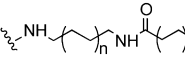
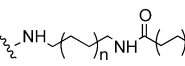
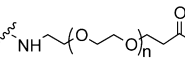
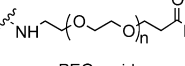
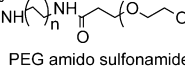
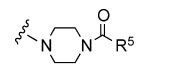
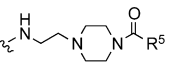
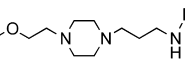
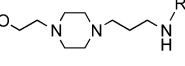
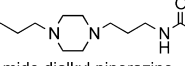
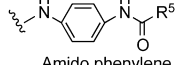
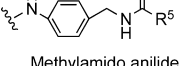
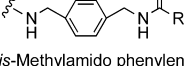
Cyclooxygenase (COX) isozymes catalyze the biotransformation of arachidonic acid into a wide variety of prostaglandins that are important biological mediators of inflammatory diseases.¹² COX-1 is constitutively expressed in most normal tissues, where it modulates housekeeping functions, such as hemostasis, vascular tone, and cytoprotection of the gastric mucosa.¹³ COX-2 is absent or expressed at very low levels in most epithelial cells but is found at high levels in inflammatory lesions and many premalignant and malignant tumors. COX-2 mRNA is detected in the early stages of tumorigenesis, such as adenomatous polyps in the colon or Barrett's esophagus.^{16–19} COX-2 expression promotes tumor growth, angiogenesis, and metastasis of cancer cells.^{14,15} Recent work has shown that selective COX-2 inhibitors are useful in the prophylaxis of various human cancers.^{20,21}

The high level of COX-2 in premalignant and malignant tumors compared to surrounding normal tissue suggests that it

Received: December 29, 2012

Revised: March 9, 2013

Published: March 15, 2013

Inhibitors	R ¹ (linker groups) ¹		R ⁵ (Fluorophore groups)
	Alkyl or PEG	Piperazine or Phenylene	
 <p>Indomethacin (R¹ = OH, R² = CH₃, R³ = Cl, R⁴ = CH₃) Iodoindomethacin (R¹ = OH, R² = CH₃, R³ = I, R⁴ = CH₃) O-DM-indomethacin (R¹ = OH, R² = CH₃, R³ = Cl, R⁴ = H) 2-DM-indomethacin (R¹ = OH, R² = H, R³ = Cl, R⁴ = CH₃)</p>  <p>11-Deoxyindomethacin (R¹ = CO₂H, R² = Cl) Reverse indomethacin (R¹ = CH₂NH₂, R² = Br)</p>  <p>Celecoxib analogs (R¹ = OH, R² = NH₂ or CH₃)</p>  <p>Flurbiprofen (R¹ = OH, R² = F, R³ = Ph) Ketoprofen (R¹ = OH, R² = PhCO, R³ = H)</p>	 <p>Amido alkyl</p>  <p>Sulfonamido alkyl</p>  <p>Thiuronium alkyl</p>  <p>Amidoalkyl sulfonamide</p>  <p>Amino alkylamide</p>  <p>PEG ester</p>  <p>PEG amide</p>  <p>PEG amido sulfonamide</p>	 <p>Amido piperazine</p>  <p>Amido alkyl piperazine</p>  <p>Acetamido dialkyl piperazinyl ether</p>  <p>Amino dialkyl piperazine</p>  <p>Amido dialkyl piperazine</p>  <p>Amido phenylene</p>  <p>Methylamido anilide</p>  <p>bis-Methylamido phenylene</p>	<p>Blue and Green Fluorophores</p> <p>Coumarin 7-diethylaminocoumarin <i>N,N</i>-Dimethylamino cinnamic acid Sulfathiazole Sulfadimethoxane Micophenolic acid Biotinyl Dansyl Dabsyl NBD Fluorescein Difluorofluorescein (Oregon green)</p> <p>Red Fluorophores</p> <p>Alexa Fluor 555 Tetramethylcarboxyrhodamine <i>bis</i>-iodobenzylcarboxyrhodamine Tetraethylsulforhodamine 5-Carboxy-X-rhodamine (5-ROX) 6-Carboxy-X-rhodamine (6-ROX) Octamethyl-5-carboxy-X-rhodamine Octamethyl-6-carboxy-X-rhodamine <i>bis</i>-Methylpentenyl-5-carboxyrhodamine</p> <p>NIR Fluorophores</p> <p>Nile blue Cy5 Cy7 NIR641 NIR664 NIR667 NIR700 NIR782 IRDye800</p> <p>Lanthanide Chelators</p> <p>DOTA Gadolinium DOTA Europium QM DOTA</p>

¹n = 0, 1, 2

Figure 1. Fluorescent COX-2 probes. Carboxylic acid containing core NSAIDs, COXIBs, or their derivatives were used as building blocks for conjugate chemistry. These compounds were tethered through a series of alkyl, piperazine, and other linkers to a diverse range of fluorophore moieties to synthesize fluorescent conjugates as COX-2-selective fluorescent imaging agents.

is an ideal target for molecular imaging by radiolabeled or fluorescent COX-2 inhibitors. To test this hypothesis, we and other laboratories have studied imaging of COX-2 expression in inflammation and cancer using ¹²³I- or ¹⁸F-labeled COX-2 selective inhibitors.^{22–26} In addition, we recently described a conjugate-based conversion of the nonsteroidal anti-inflammatory drug (NSAID), indomethacin, into fluorescent carboxy-X-rhodamine (ROX) conjugates that are capable of inhibiting COX-2 selectively and potently in both purified protein and intact cells. These conjugates, which do not significantly inhibit COX-1, enabled the optical imaging of COX-2 in inflammatory lesions and COX-2-expressing tumors in vivo.²⁷ The present paper describes the details of the structure–activity relationship (SAR) studies performed for optimization of these lead compounds from a wide range of fluorescent conjugates of NSAIDs or COX-2-selective inhibitors (COXIBs). The conjugates were evaluated as COX-2-targeted imaging agents, and active molecules were validated in vitro and in vivo as COX-2-targeted agents in cells and tumors. The results provide critical background and further support for our previous report,²⁷ which reveals the first fluorescently labeled optical imaging agent validated for COX-2-targeted in vivo imaging of inflammation and cancer.

EXPERIMENTAL PROCEDURES

Chemistry. Standard methods were utilized for the synthesis of fluorescent derivatives of NSAIDs and COXIBs. A wide variety of carboxylic acid-containing core compounds (e.g., indomethacin, an iodoindomethacin, an indolyl carboxamide analog of indomethacin (reverse indomethacin), flurbiprofen, ketoprofen, or a carboxylic acid derivative of celecoxib) were tethered through a series of alkyl, aryl piperazinyl, or polyethylene glycol linkers to a diverse range of bulky organic fluorophore moieties. The fluorophores included dansyl, dabsyl, coumarin, fluorescein, rhodamine, alexa-fluor, nile blue, cy5, cy7, near IR, and IR dyes, as well as some lanthanide chelators (Figure 1). Synthetic procedures, in addition to analytical and spectroscopic characterization of all compounds, are described in Supporting Information.

Fluorometry. Steady state fluorescence excitation and emission spectra were determined for each compound with a Spex 1681 Fluorolog spectrofluorometer, equipped with a 450 W xenon arc lamp. The excitation and emission monochromator slit widths were 1–2 mm. The solvent used was pH 7 buffer.

Inhibition Assay Using Purified COX-1 and COX-2. Inhibition of purified ovine COX-1 or mouse COX-2 by test compounds was assayed by a previously described method,²⁷ which quantifies the conversion of [¹⁻¹⁴C]arachidonic acid to

[1-¹⁴C]prostaglandin products. Reaction mixtures of 200 μ L consisted of hematin-reconstituted protein in 100 mM Tris-HCl, pH 8.0, 500 μ M phenol, and [1-¹⁴C]arachidonic acid (50 μ M, \sim 55–57 mCi/mmol, Perkin-Elmer). For the time-dependent inhibition assay, hematin-reconstituted COX-1 (44 nM) or COX-2 (66 nM) was preincubated at 25 $^{\circ}$ C for 17 min and 37 $^{\circ}$ C for 3 min with varying inhibitor concentrations in dimethylsulfoxide followed by the addition of [1-¹⁴C]arachidonic acid (50 μ M) for 30 s at 37 $^{\circ}$ C. Reactions were terminated by solvent extraction in diethyl ether/methanol/1 M citrate buffer, pH 4.0 (30:4:1). The phases were separated by centrifugation at 2000g for 2 min, and the organic phase was spotted on a thin-layer chromatography plate (EMD Kiesegel 60, VWR). The plate was developed in ethyl acetate/methylene chloride/glacial AcOH (75:25:1) at 4 $^{\circ}$ C. Radiolabeled products were quantified with a radioactivity scanner (Bioscan, Inc., Washington, DC). The percentage of total products observed at different inhibitor concentrations was divided by the percentage of products observed for protein samples preincubated for the same time with dimethyl sulfoxide.

Cell Culture and In Vitro Intact Cell Metabolism

Assay. Inhibition of COX-2 in intact cells by test compounds was assayed by a previously described method.²⁷ Briefly, RAW264.7, ATCC TIB-71 murine macrophage-like cells (passage number 8–15, mycoplasma negative by a polymerase chain reaction detection method) were grown in Dulbecco's Modified Eagle Medium (DMEM) + 10% heat-inactivated fetal bovine serum to 40% confluence (6-well plates, Sarstedt). The cells were activated for 7 h in 2 mL serum-free DMEM with 200 ng/mL bacterial lipopolysaccharide (Calbiochem) and 10 U/mL interferon gamma (Calbiochem) to induce COX-2 expression. Human 1483 head and neck squamous cell carcinoma (HNSCC) cells (passage 8–18, mycoplasma negative by a polymerase chain reaction detection method) were cultured in DMEM/F12 + 10% fetal bovine serum + antibiotic/antimycotic in 6-well plates to 60% confluence. Serum-free medium (2 mL) was added, and the cells were treated with inhibitor dissolved in DMSO (0–5 μ M, final concentration) for 30 min at 37 $^{\circ}$ C followed by the addition of [1-¹⁴C]-arachidonic acid [10 μ M, \sim 55 mCi/mmol] for 20 min at 37 $^{\circ}$ C. Reactions were terminated and analyzed by thin layer chromatography as described above.

Fluorescence Microscopy of 1483 HNSCC Cells. Fluorescence imaging of human 1483 HNSCC cells by compound **58** was performed by a previously described method.²⁷ Briefly, human 1483 HNSCC cells were grown to 60% confluence. The cells were incubated in 2.0 mL Hank's balanced salt solution (HBSS)/Tyrode's with 200 nM compound **58** for 30 min at 37 $^{\circ}$ C. The cells were then washed briefly three times and incubated in HBSS/Tyrode's for 30 min at 37 $^{\circ}$ C. Following the required washout period, the cells were imaged in 2.0 mL fresh HBSS/Tyrode's on a Zeiss Axiovert 25 Microscope with the propidium iodide filter (0.5–1.0 s exposure, gain of 2). All treatments were performed in duplicate dishes in at least three separate experiments. To block the COX-2 active site, the cells were preincubated with 5 or 10 μ M indomethacin for 20 min prior to the addition of the test compound.

Establishment of Xenograft Tumors in Nude Mice.

Human 1483 HNSCC cells and HCT116 colorectal carcinoma cells were used to grow tumor xenografts in nude mice using a previously described method.²⁷ Female nude mice, NU-Fox1nu, were purchased at 6–7 weeks of age from Charles

River Laboratories. Human 1483 HNSCC cells and HCT116 colorectal carcinoma cells were trypsinized and resuspended in cold PBS containing 30% Matrigel such that 1×10^6 cells in 100 μ L were injected subcutaneously on the left flank. The HCT116 and 1483 xenografts required only 2–3 weeks of growth.

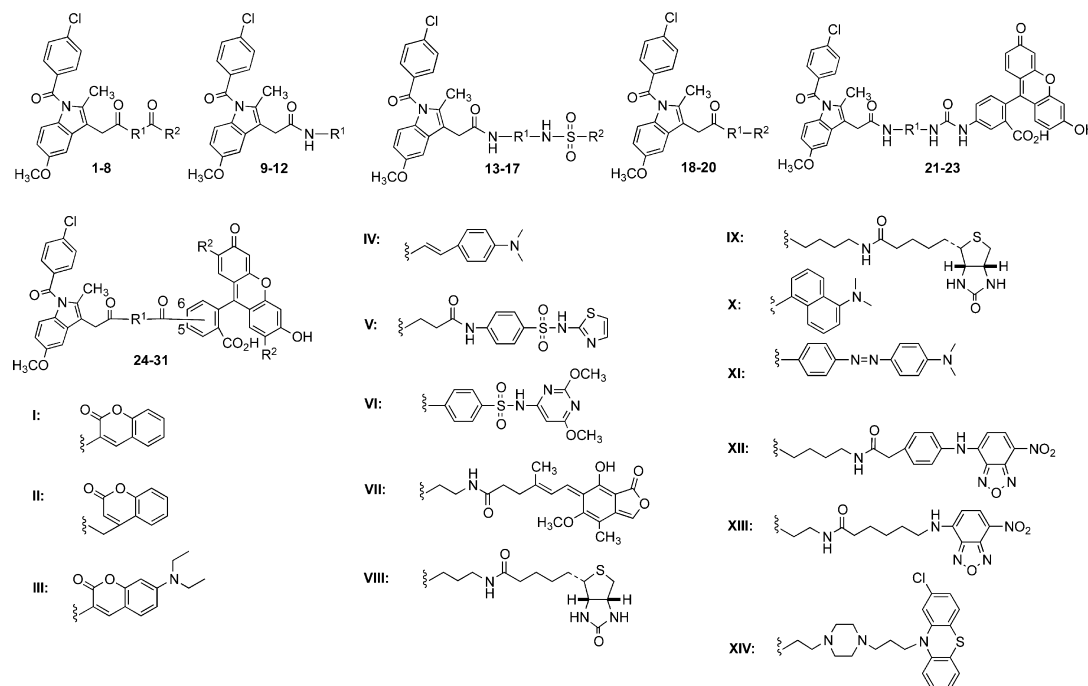
In Vivo Imaging of Nude Mice with Xenografts.

Fluorescence imaging of tumors by test compounds was performed by a previously described method.²⁷ Female nude mice bearing medium-sized 1483 or HCT116 xenograft tumors on the left flank were dosed by intraperitoneal injection with 2 mg/kg compound **58**. The animals were lightly anesthetized with 2% isoflurane for fluorescence imaging in the Xenogen IVIS 200 with the DSRed filter at 1.5 cm depth and 1 s exposure (f2).

RESULTS

Synthesis of Fluorescent COX-2 Inhibitors. The synthesis of NSAID- or COXIB-diamide imaging agents targeted to COX-2 first required the conjugation of the carboxylate functional group of the NSAID or COXIB nucleus to a diamine linker. Diamide linkages were chosen rather than mixed amide-ester linkages to minimize the potential for hydrolysis in intact cells or in vivo. Selective amidation of only one of the two available amino groups present in the diamine tether necessitated protection of one of the groups. This was accomplished by the use of the mono *tert*-butoxycarbonyl (BOC)-protected alkyl diamine. Reaction of indomethacin with a series of mono BOC-alkyl diamines in the presence of ethyl-1-[3-(dimethylamino)propyl]-3-ethylcarbodiimide followed by treatment with HCl (gas) gave the corresponding indomethacin-alkylamine hydrochloride salts in high yield. Similarly, indomethacin-piperazine hydrochloride and indomethacin-phenylenediamine hydrochloride were synthesized by substituting mono BOC-alkyl diamine with mono BOC-piperazine or mono BOC-phenylenediamine, respectively. For synthesizing indomethacin-polyethylene glycolyl (PEG) carboxylic acid, *t*-butyl-PEG4-amine was used in place of mono BOC-alkyl diamine, followed by deprotection with trifluoroacetic acid at room temperature. As described above, other NSAIDs, COXIBs, or appropriate analogs were linked to a chosen tether (alkyl diamine, PEG, piperazine, or phenylene diamine) to form the corresponding conjugates having a terminal primary or secondary amine or a carboxylic acid group. The isothiocyanate, sulfonyl chloride, or succinimidyl ester of the desired fluorophore was conjugated with the amino group of the tether-linked-NSAID or -COXIB using triethylamine as a base. Alternatively, formation of a carboxylamide from the reaction of a carboxylic acid with an amino-group required either ethyl-1-[3-(dimethylamino)propyl]-3-ethylcarbodiimide or *N,N,N,N*-tetramethyl-*O*-(*N*-succinimidyl)uronium tetrafluoroborate coupling reactions. Using this general strategy, 5-ROX-acid was activated using *N,N,N,N*-tetramethyl-*O*-(*N*-succinimidyl)uronium tetrafluoroborate in the presence of triethylamine at room temperature and coupled with the free amino group of the tether-linked-NSAIDs or COXIBs to afford the target fluorescent conjugates. All other fluorescent dyes were conjugated with the respective NSAID or COXIB scaffolds using a similar coupling strategy in good yields (60–70%). The structure of all compounds was established by NMR and mass spectrometry. HPLC analyses in two different solvent systems of all representative fluorescent compounds indicated a minimum purity of 96.0%. Most of the compounds were in

Table 1. In Vitro Purified COX-1 and COX-2 Enzyme Inhibition Assay Data of Compounds 1–31



No	R ¹	R ²	Isomer	IC ₅₀ (μM) ^a	
				COX-1	COX-2
1	-(CH ₂) ₂ -	I	-	> 4	0.78
2	-(CH ₂) ₃ -	I	-	> 4	0.60
3	-(CH ₂) ₂ -	II	-	> 4	> 4
4	-(CH ₂) ₃ -	III	-	> 4	0.05
5	-(CH ₂) ₄ -	III	-	> 4	0.03
6	-(CH ₂) ₂ -	IV	-	> 4	0.51
7	-(CH ₂) ₄ -	V	-	> 4	0.96
8	-N(CH ₂) ₂ -	V	-	> 4	> 4
9	VI	-	-	0.08	0.14
10	VII	-	-	> 4	> 4
11	VII	-	-	> 4	> 4
12	IX	-	-	> 4	1.30
13	-(CH ₂) ₂ -	X	-	> 4	0.06
14	-(CH ₂) ₃ -	X	-	> 4	0.07
15	-(CH ₂) ₄ -	X	-	> 4	0.06
16	-(CH ₂) ₂ -	XI	-	> 4	0.08
17	-(CH ₂) ₃ -	XI	-	0.21	0.13
18	NH	XII	-	> 4	0.50
19	NH	XIII	-	> 4	> 4
20	O	XIV	-	> 4	> 4
21	-(CH ₂) ₂ -	-	-	> 4	> 4
22	-(CH ₂) ₃ -	-	-	> 4	> 4
23	-(CH ₂) ₄ -	-	-	> 4	3.10
24	-NH-(CH ₂) ₄ -NH-	H	5	> 4	> 4
25	-NH-(CH ₂) ₄ -NH-	H	6	> 4	> 4
26	-NH-(CH ₂) ₄ -NH-CO-(CH ₂) ₅ -NH-	H	5	> 4	> 4
27	-NH-(CH ₂) ₄ -NH-	F	6	> 4	3.20
28	-NH-(CH ₂) ₄ -NH-CO-(CH ₂) ₅ -NH-	F	6	> 4	2.90
29	-N(CH ₂) ₂ -	H	6	> 4	> 4
30	-N(CH ₂) ₂ -	H	6	> 4	> 4
31	-N(CH ₂) ₂ -	H	6	> 4	> 4

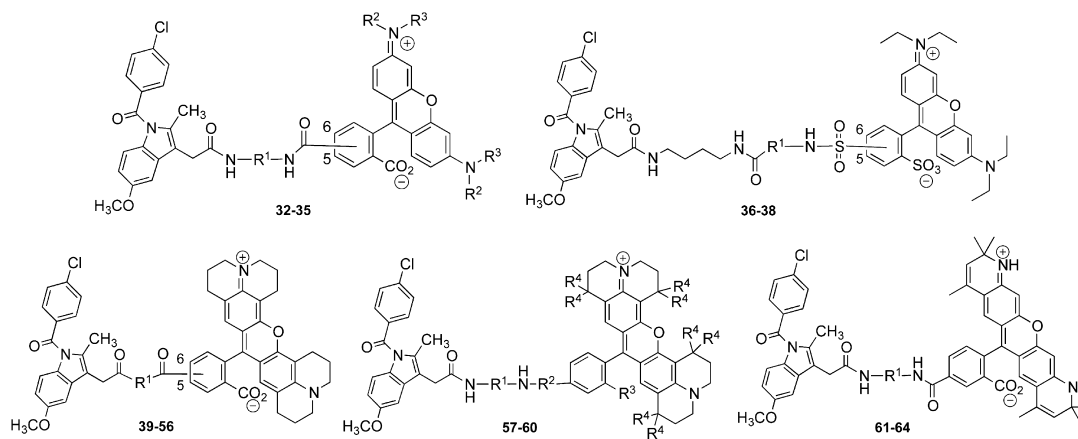
^aIC₅₀ values were determined as described in Experimental Procedures. Assays were run in duplicate.

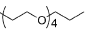
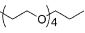
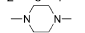
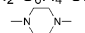
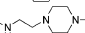
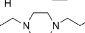
excess of 98.5% purity. The synthetic procedure and compound characterization are described in detail in Supporting Information.

Evaluation of Fluorescent COX-2 Inhibitors Using Purified Enzymes. The inhibitory activity of test compounds against ovine COX-1 or mouse COX-2 was evaluated by a thin layer chromatography assay,²⁷ as briefly described in Experimental Procedures.

Indomethacin Conjugates of Blue and Green Fluorophores. IC₅₀ values for the inhibition of purified COX enzymes by test compounds are listed in Table 1. Compound 1, a conjugate of indomethacin and coumarin tethered through an ethylenediamide linker, displayed selective COX-2 inhibition (Table 1). Chain length extension of the linker group of 1 to higher alkyl homologues or replacement of coumarin with 7-diethylaminocoumarin revealed significant increases in potency

Table 2. In Vitro Purified COX-1 and COX-2 Enzyme Inhibition Assay Data of Compounds 32–64



No	R ¹	R ²	R ³	R ⁴	Isomer	IC ₅₀ (μM) ^a	
						COX-1	COX-2
32	-(CH ₂) ₄ -	H	H	-	6	> 4	> 4
33	-(CH ₂) ₃ -	CH ₃	CH ₃	-	6	> 4	3.9
34	-(CH ₂) ₄ -	CH ₃	CH ₃	-	6	> 4	> 4
35	-(CH ₂) ₄ -	-CH ₂ -C ₆ H ₄ -I	CH ₃	-	5	> 4	> 4
36		-	-	-	5	> 4	0.16
37		-	-	-	6	> 4	1.10
38	-(CH ₂) ₅ -	-	-	-	5	> 4	1.20
39	-NH-(CH ₂) ₂ -NH-	-	-	-	5	> 4	2.80
40	-NH-(CH ₂) ₃ -NH-	-	-	-	5	1.20	1.50
41	-NH-(CH ₂) ₄ -NH-	-	-	-	5	> 4	0.70
42	-NH-(CH ₂) ₅ -NH-	-	-	-	5	> 4	0.94
43	-NH-(CH ₂) ₆ -NH-	-	-	-	5	> 4	1.70
44	-NH-C ₆ H ₄ -CH ₂ -NH-	-	-	-	5	> 4	0.50
45	-NH-CH ₂ -C ₆ H ₄ -CH ₂ -NH-	-	-	-	5	> 4	0.60
46		-	-	-	5	> 4	1.30
47	-NH-(CH ₂) ₂ -NH-	-	-	-	6	> 4	> 4
48	-NH-(CH ₂) ₃ -NH-	-	-	-	6	> 4	> 4
49	-NH-(CH ₂) ₄ -NH-	-	-	-	6	> 4	0.83
50	-NH-(CH ₂) ₅ -NH-	-	-	-	6	> 4	> 4
51	-NH-C ₆ H ₄ -NH-	-	-	-	6	> 4	0.32
52	-NH-C ₆ H ₄ -CH ₂ -NH-	-	-	-	6	> 4	1.20
53	-NH-CH ₂ -C ₆ H ₄ -CH ₂ -NH-	-	-	-	6	> 4	0.63
54		-	-	-	6	> 4	> 4
55		-	-	-	6	> 4	> 4
56		-	-	-	6	> 4	> 4
57	-(CH ₂) ₃ -	CO	CO ₂ ⁻	CH ₃	5	> 4	> 4
58	-(CH ₂) ₄ -	CO	CO ₂ ⁻	CH ₃	5	> 4	1.40
59	-CH ₂ -C ₆ H ₄ -CH ₂ -	CO	CO ₂ ⁻	CH ₃	5	> 4	> 4
60	-(CH ₂) ₄ -	SO ₂	SO ₃ ⁻	H	5	> 4	> 4
61	-(CH ₂) ₂ -	-	-	-	5	> 4	> 4
62	-(CH ₂) ₃ -	-	-	-	5	> 4	> 4
63	-(CH ₂) ₄ -	-	-	-	5	> 4	> 4
64	-CH ₂ -C ₆ H ₄ -CH ₂ -	-	-	-	5	> 4	> 4

^aIC₅₀ values were determined as described in Experimental Procedures. Assays were run in duplicate.

and selectivity against COX-2 (4–5). For example, the *n*-butyldiamide-conjugate 5 was more potent and selective as a COX-2 inhibitor than 1. Conjugation of organic functionalities (i.e., *N,N*-dimethylamino cinnamic acid, sulfathiazole, sulfadimethoxine, mycophenolic acid, or biotin) afforded a series of compounds (6–12), of which the *trans*-cinnamyl (6) or sulfathiazolyl (7) conjugates displayed potent and selective COX-2 inhibition. Compared to compounds 6 or 7, the dansyl (13–15) or dabsyl (16–17) derivatives were more potent and selective for COX-2 inhibition (13, λ_{ex} = 355 nm, λ_{em} = 493 nm). The *n*-butyldiamide-tethered nitrobenzoxadiazole (NBD)-conjugate (18) also displayed selective COX-2 inhibition. However, shortening of the alkyl chain or incorporation of perphenazine with compounds 19 and 20 showed complete loss of COX inhibitory activity (20, λ_{ex} = 492 nm, λ_{em} = 505 nm).

Although a similar loss of COX activity was observed with fluorescein-conjugates (e.g., 21, 22, 24–26, 29–31), compounds 23, 27, and 28 displayed COX-2 inhibitory activity to some extent. These results suggested that transformation of indomethacin into fluorescent conjugates can lead to selective COX-2 inhibition; however, the length and nature of the tether and the structure of the fluorophore have a significant impact on the COX inhibitory potential of the conjugates.

Indomethacin Conjugates of Red Fluorophores. The fluorescent derivatives of indomethacin with alexa fluor, tetramethylrhodamine, or *bis*-iodobenzylcarboxyrhodamine (compounds 32–35) showed no COX inhibitory activity, even at the higher concentrations (Table 2). However, COX-2 inhibitory activity was achieved with the PEG-containing tetraethyl 5- or 6-sulforhodamine conjugates 36 and 37. Poor

Table 3. In Vitro Purified COX-1 and COX-2 Enzyme Inhibition Assay Data of Compounds 65–84

65-84

I:

VI:

II:

VII:

III:

VIII:

IV:

IX:

V:

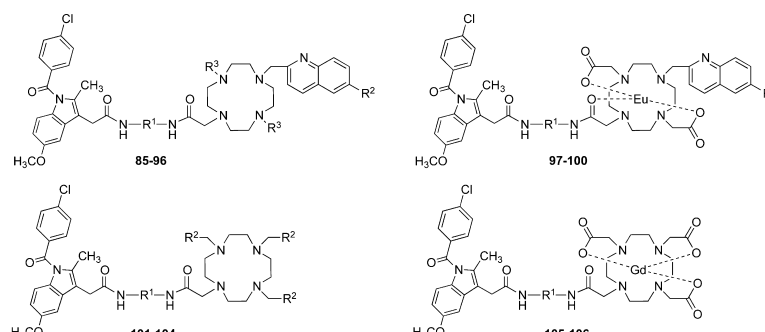
No	R ¹	R ²	IC ₅₀ (μM) ^a	
			COX-1	COX-2
65		I	> 4	1.70
66	-HN-(CH ₂) ₄ -NH-	II	> 4	> 4
67	-HN-(CH ₂) ₄ -NH-	III	> 4	1.40
68	-HN-(CH ₂) ₄ -NH-	IV	3.40	0.50
69	-HN-(CH ₂) ₂ -NH-	V	> 4	> 4
70	-HN-(CH ₂) ₃ -NH-	V	> 4	> 4
71		V	3	3
72	-HN-(CH ₂) ₅ -NH-	V	> 4	> 4
73	-HN-(CH ₂) ₆ -NH-	V	> 4	> 4
74	-HN-(CH ₂) ₂ -NH-	VI	> 4	> 4
75	-HN-(CH ₂) ₃ -NH-	VI	> 4	> 4
76	-HN-(CH ₂) ₄ -NH-	VI	> 4	> 4
77	-HN-(CH ₂) ₅ -NH-	VI	> 4	> 4
78	-HN-(CH ₂) ₆ -NH-	VI	> 4	> 4
79	-HN-(CH ₂) ₄ -NH-	VII	> 4	1.00
80	-HN-(CH ₂) ₅ -NH-	VII	> 4	> 4
81	-HN-(CH ₂) ₆ -NH-	VII	> 4	> 4
82	-HN-C ₂ H ₄ -CH ₂ -NH-	VII	> 4	1.80
83	-HN-(CH ₂) ₄ -NH-	VIII	> 4	> 4
84	-HN-(CH ₂) ₄ -NH-	IX	> 4	> 4

^aIC₅₀ values were determined as described in Experimental Procedures. Assays were run in duplicate.

COX inhibition was observed with **38** having an *n*-pentylsulfonamido *n*-butyldiamide linker (**36**, λ_{ex} = 571 nm, λ_{em} = 593 nm). Selective COX-2 inhibition by the 5- or 6-ROX derivatives was extremely sensitive to the length and electronic properties of the linker moieties. For instance, the 5-ROX conjugate **39**, containing an ethylenediamide linker, was a weak inhibitor of COX-2. As the alkyl chain length increased, COX-2 inhibitory potency and selectivity increased substantially, with the *n*-butyldiamide derivative **41** (Fluorocoxib A, λ_{ex} = 580 nm, λ_{em} = 605 nm) exhibiting the best combination of COX-2 inhibitory potency and selectivity and identified as one of the most potent derivatives in the series.²⁷ A further increase in alkyl chain length resulted in a dramatic reduction in COX-2 inhibitory

potency (e.g., **42** and **43**). Interestingly, the phenylene derivatives **44** and **45** showed similar potencies to **41**. Replacement of the *n*-butyldiamide linker of compound **41** with a piperazine linker yielded a very weak inhibitor (**46**) of COX-2. Likewise, indomethacin-6-ROX conjugates (**47–56**), linked through alkyl, piperazine, or phenylene tethers, showed similar potencies to those of the corresponding 5-ROX conjugates. Notably, the regioisomer **49** (Fluorocoxib B, λ_{ex} = 581 nm, λ_{em} = 603 nm) exhibited selective COX-2 inhibition.²⁷ However, fluorescent conjugates **57–64**, containing bulkier rhodamine dyes, showed significantly lower potency or complete loss of COX-2 inhibitory activity with the exception of compound **58** (λ_{ex} = 572 nm, λ_{em} = 595 nm), which

Table 4. In Vitro Purified COX-1 and COX-2 Enzyme Inhibition Assay Data of Compounds 85–106



No	R ¹	R ²	R ³	IC ₅₀ (μM) ^a	
				COX-1	COX-2
85	-(CH ₂) ₂ -	CH ₃	H	> 4	> 4
86	-(CH ₂) ₄ -	CH ₃	H	> 4	> 4
87	-(CH ₂) ₂ -	F	H	> 4	> 4
88	-(CH ₂) ₄ -	F	H	> 4	> 4
89	-(CH ₂) ₂ -	CH ₃	-CH ₂ CO ₂ t-Bu	> 4	> 4
90	-(CH ₂) ₄ -	CH ₃	-CH ₂ CO ₂ t-Bu	> 4	> 4
91	-(CH ₂) ₂ -	F	-CH ₂ CO ₂ t-Bu	> 4	> 4
92	-(CH ₂) ₄ -	F	-CH ₂ CO ₂ t-Bu	> 4	> 4
93	-(CH ₂) ₂ -	CH ₃	-CH ₂ CO ₂ H	> 4	> 4
94	-(CH ₂) ₄ -	CH ₃	-CH ₂ CO ₂ H	> 4	> 4
95	-(CH ₂) ₂ -	F	-CH ₂ CO ₂ H	> 4	> 4
96	-(CH ₂) ₄ -	F	-CH ₂ CO ₂ H	> 4	> 4
97	-(CH ₂) ₂ -	CH ₃	-	> 4	> 4
98	-(CH ₂) ₄ -	CH ₃	-	> 4	> 4
99	-(CH ₂) ₂ -	F	-	> 4	> 4
100	-(CH ₂) ₄ -	F	-	> 4	> 4
101	-(CH ₂) ₂ -	-CH ₂ CO ₂ t-Bu	-	> 4	> 4
102	-(CH ₂) ₄ -	-CH ₂ CO ₂ t-Bu	-	> 4	> 4
103	-(CH ₂) ₂ -	-CH ₂ CO ₂ H	-	> 4	> 4
104	-(CH ₂) ₄ -	-CH ₂ CO ₂ H	-	> 4	> 4
105	-(CH ₂) ₂ -	-	-	> 4	> 4
106	-(CH ₂) ₄ -	-	-	> 4	> 4

^aIC₅₀ values were determined as described in Experimental Procedures. Assays were run in duplicate.

displayed activity comparable to the 5- and 6-ROX conjugates. In summary, a four-carbon *n*-alkyl linker with 5- or 6-ROX provided the best balance for COX-2 inhibitory activity and selectivity of the fluorescent indomethacin conjugates.

Indomethacin Conjugates of NIR Fluorophores. Conjugation of a Nile blue dye with the carboxylic acid moiety of indomethacin tethered through a PEG4 linker afforded compound **65** ($\lambda_{\text{ex}} = 618$ nm, $\lambda_{\text{em}} = 670$ nm), a perchlorate salt, which was identified as a poor COX-2 inhibitor (Table 3). A complete loss of COX inhibitory activity was observed with the Cy5 conjugate **66**. Interestingly, the Cy7 conjugate **67** inhibited COX-2 with poor potency, while inhibitory activity but lack of selectivity was observed with the NIR641 conjugate (**68**), a chloride salt. No significant COX-2 inhibition was discernible with the ethyl- or propyldiamide-linked indomethacin conjugates of NIR664, such as compounds **69** and **70**, respectively. Nonselective COX inhibition was observed with the piperazine-linked conjugate **71**, an inner salt (zwitterion). However, a complete loss of COX activity was documented with the higher alkyl homologues (**72**, **73**). A similar loss was observed with the NIR667 conjugates **74–78** (chloride salts). Conjugation of indomethacin with NIR700, an inner salt, afforded the selective COX-2 inhibitor **79** ($\lambda_{\text{ex}} = 710$ nm, $\lambda_{\text{em}} = 731$ nm), which contained an *n*-butyldiamide linker. When the length of the linker was increased, conjugates **80–81** showed a dramatic loss of COX-2 inhibitory activity. Interestingly, a poor potency was achieved when the *n*-butyl linker was replaced by a phenylene-alkyl hybrid linker in compound **82**, and no COX-2 inhibition was observed with the NIR782 or IRDye800

derivatives, compounds **83** and **84**, respectively. A similar lack of activity was observed with DOTA-, Eu-Quinoline(F)-DOTA-, Eu-Quinoline(CH₃)-DOTA-, or Gd-DOTA-derivatives (compounds **85–106**), even at very high concentrations (Table 4). Thus, conjugation of indomethacin with a zwitterionic fluorophore tethered through an *n*-butyldiamide linker is most suitable to achieve COX-2 inhibitory activity. Highly polar organic functional groups, such as DOTA, or its analogous lanthanide chelators, are not suitable for COX-2 inhibitory activity of the conjugates.

Fluorescent Conjugates of Miscellaneous NSAIDs and COXIBs. Lack of isoform selectivity or complete loss of COX-2 inhibitory activity was often observed with fluorescent conjugates of NSAIDs and COXIBs other than indomethacin (Table 5). For instance, the iodoindomethacin-5-ROX conjugates **107** and **109** showed no COX-2 selectivity. A complete loss of COX inhibitory activity was observed with the 5-ROX or NIR664 conjugates **108**, **110**, and **111**. We synthesized *O*-des-methyl- or 2-des-methyl-indomethacin-5-ROX conjugates **112** and **113**, which were selective COX-2 inhibitors. However, the 2-des-methyl-, *N*-des-4-chlorobenzoyl-, or *N*-4-chlorobenzyl-indomethacin and 5- or 6-ROX conjugates **114–117**, containing an *n*-butyldiamide linker, showed no COX-2 inhibition. A loss of COX-2 inhibitory activity was also observed with fluorescent derivatives of *reverse*-indomethacin, **118–122**. An exception was identified with the *reverse*-indomethacin-NIR700 conjugate (**123**), which exhibited selective COX-2 inhibition with a moderate potency. A complete loss of COX-2 inhibitory activity was observed with the majority of fluorescent derivatives of celecoxib, flurbiprofen,

Table 5. In Vitro Purified COX-1 and COX-2 Enzyme Inhibition Assay Data of Compounds 107–123

I:

III:

V:

II:

IV:

VI:

No	R ¹	R ²	R ³	R ⁴	R ⁵	IC ₅₀ (μM) ^a	
						COX-1	COX-2
107	-CO-C ₆ H ₄ -I	CH ₃	OCH ₃	-(CH ₂) ₂ -	I	0.99	0.91
108	-CO-C ₆ H ₄ -I	CH ₃	OCH ₃	-(CH ₂) ₄ -	I	> 4	> 4
109	-CO-C ₆ H ₄ -I	CH ₃	OCH ₃	-C ₆ H ₄ -CH ₂ -	I	1.60	0.64
110	-CO-C ₆ H ₄ -I	CH ₃	OCH ₃	-(CH ₂) ₄ -	II	> 4	> 4
111	-CO-C ₆ H ₄ -I	CH ₃	OCH ₃	-(CH ₂) ₅ -	I	> 4	> 4
112	-CO-C ₆ H ₄ -Cl	CH ₃	OH	-(CH ₂) ₄ -	I	> 4	0.59
113	-CO-C ₆ H ₄ -Cl	H	OCH ₃	-(CH ₂) ₂ -	I	> 4	1.80
114	-CO-C ₆ H ₄ -Cl	H	OCH ₃	-(CH ₂) ₄ -	I	> 4	> 4
115	H	CH ₃	OCH ₃	-(CH ₂) ₄ -	I	> 4	> 4
116	-CH ₂ -C ₆ H ₄ -Cl	CH ₃	OCH ₃	-(CH ₂) ₄ -	I	> 4	> 4
117	-CH ₂ -C ₆ H ₄ -Cl	CH ₃	OCH ₃	-(CH ₂) ₄ -	III	> 4	> 4
118	-CH ₂ -C ₆ H ₄ -Br	CH ₃	OCH ₃	-	IV	> 4	> 4
119	-CH ₂ -C ₆ H ₄ -Br	CH ₃	OCH ₃	-	V	> 4	> 4
120	-CH ₂ -C ₆ H ₄ -Br	CH ₃	OCH ₃	-	VI	> 4	> 4
121	-CH ₂ -C ₆ H ₄ -Br	CH ₃	OCH ₃	-	III	> 4	> 4
122	-CH ₂ -C ₆ H ₄ -Br	CH ₃	OCH ₃	-	I	> 4	> 4
123	-CH ₂ -C ₆ H ₄ -Br	CH ₃	OCH ₃	-	II	> 4	0.48

^aIC₅₀ values were determined as described in Experimental Procedures. Assays were run in duplicate.

or ketoprofen (compounds 124–139). However, conjugation of the celecoxib analog with Nile Blue or sulforhodamine (e.g., 124 and 125) resulted in selective COX-2 inhibition with moderate to poor potencies. The COX-2 inhibitory activity of indomethacin- or celecoxib-like building blocks (140–152) is delineated in Table 6. Although the derivatives of indomethacin and celecoxib, such as iodoindomethacin and carboxypropionyl celecoxib, retain the COX-2 inhibitory activity of the parent compound, their fluorescent derivatives were not always COX-2 inhibitors. So, unlike the parent indomethacin, conversion of indomethacin- or celecoxib-like molecules into fluorescent amide derivatives does not readily generate a family of highly selective COX-2 inhibitors.

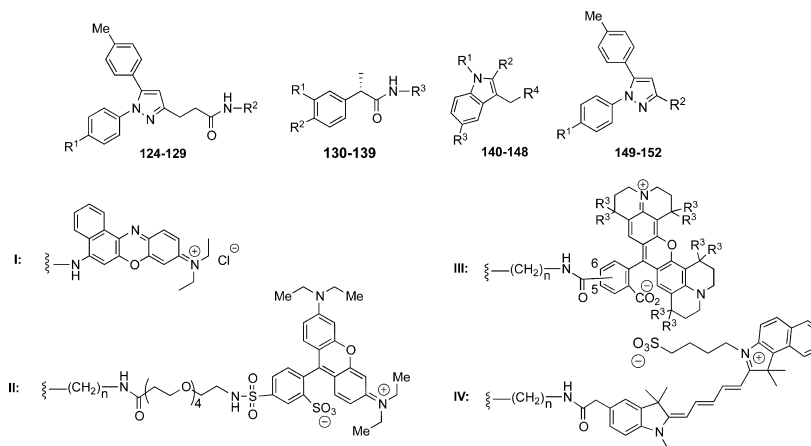
Evaluation of Fluorescent COX-2 Inhibitors in Cell Culture. The ability of fluorescent derivatives to inhibit COX-2 in intact cells was assayed in activated RAW264.7 macrophages or 1483 HNSCC cells using previously reported methods,²⁷ as briefly described in Experimental Procedures. In this assay, many of the structurally diverse fluorescent compounds inhibited COX-2 in LPS-activated RAW264.7 cells with IC₅₀ values in the nanomolar range (Table 7). For instance, the IC₅₀ values for inhibition of prostaglandin synthesis by 41 and 58, were 0.31 and 0.34, μM, respectively. In 1483 HNSCC cells, which constitutively express COX-2, compounds 41 and 58 retained their COX-2 inhibitory activity with IC₅₀ values of 0.09 and 0.38 μM, respectively. Thus, conjugation of an NSAID, indomethacin, with zwitterionic fluorophores, tethered through an *n*-butyldiamide linker afforded fluorescent conjugates that were capable of passing through the cell membrane to inhibit COX-2 effectively.

In Vitro Optical Imaging of Cells. The human head and neck cancer cell line, 1483, which expresses high levels of

COX-2,²⁸ was treated with compound 58. After washout, the cells were imaged by fluorescence microscopy and exhibited strong red fluorescence due to the accumulation of the rhodamine derivative (Figure 2A). Preincubation of the cells with the COX inhibitor indomethacin blocked uptake and labeling of 1483 cells by compound 58 (Figure 2B). These results are consistent with those reported previously for compound 41.²⁷

In Vivo Optical Imaging of Tumor Xenografts. We evaluated the ability of compound 58 to target COX-2 in human tumor xenografts. Nude mice bearing 1483 or HCT116 xenograft tumors on the left flank were dosed by intraperitoneal injection with compound 58 (2 mg/kg). At 60 min post-injection, no fluorescence was observed in the tumor. Signal was detected in the COX-2 expressing 1483 tumors starting at 3 h (Figure 3A). In contrast to the selective uptake of 58 into 1483 xenografts, minimal uptake was observed at 3 h in HCT116 xenografts, a human colon tumor that does not express COX-2.²⁹ An ex vivo imaging was performed to confirm the in vivo imaging results and to verify the 1483 tumor signal was due to the tumor uptake of 58, and not from the nearby normal tissues or skin. A bright fluorescence signal was detected in the ex vivo 1483 tumor as compared with the HCT116 tumor (Figure 3C,D). The signal enrichment of 58 in the 1483 tumors compared to HCT116 or contralateral leg muscle was established to be >10:1 (Figure 3E). Further, we performed a COX-2 blocking experiment using indomethacin, in which nude mice with 1483 xenografts were pretreated with either DMSO or indomethacin in DMSO (2 mg/kg, intraperitoneal) prior to compound 58 dosing (2 mg/kg, intraperitoneal). At 3 h postinjection, the DMSO-pretreated mice showed strong fluorescence in their tumors, as compared to weak signals in the tumors of the indomethacin-pretreated mice (SI Figure S1).

Table 6. In Vitro Purified COX-1 and COX-2 Enzyme Inhibition Assay Data of Compounds 124–152



No	R ¹	R ²	R ³	R ⁴	n	Isomer	IC ₅₀ (μM) ^a	
							COX-1	COX-2
124	SO ₂ CH ₃	I	-	-	-	-	> 4	0.82
125	SO ₂ NH ₂	II	-	-	2	-	> 25	3.98
126	SO ₂ NH ₂	III	H	-	2	6	> 4	> 4
127	SO ₂ NH ₂	III	H	-	2	5	> 4	> 4
128	SO ₂ NH ₂	III	CH ₃	-	2	5	> 4	> 4
129	SO ₂ NH ₂	IV	-	-	2	-	> 4	> 4
130	F	Ph	IV	-	2	-	> 4	> 4
131	F	Ph	IV	-	3	-	> 4	> 4
132	F	Ph	IV	-	4	-	> 4	> 4
133	F	Ph	IV	-	5	-	> 4	> 4
134	F	Ph	IV	-	6	-	> 4	> 4
135	PhCO	H	IV	-	2	-	> 4	> 4
136	PhCO	H	IV	-	3	-	> 4	> 4
137	PhCO	H	IV	-	4	-	> 4	> 4
138	PhCO	H	IV	-	5	-	> 4	> 4
139	PhCO	H	IV	-	6	-	> 4	> 4
140	-CO-C ₆ H ₄ -Cl	CH ₃	OH	CO ₂ H	-	-	0.28	0.26
141	-CO-C ₆ H ₄ -Cl	H	OCH ₃	CO ₂ H	-	-	> 4	> 4
142	-CH ₂ -C ₆ H ₄ -Cl	CH ₃	OCH ₃	CO ₂ H	-	-	> 4	> 4
143	-CH ₂ -C ₆ H ₄ -F	CH ₃	OCH ₃	CO ₂ H	-	-	> 4	> 4
144	-CH ₂ -C ₆ H ₄ -Br	CH ₃	OCH ₃	CO ₂ H	-	-	> 4	> 4
145	-CO-C ₆ H ₄ -I	CH ₃	OCH ₃	CO ₂ H	-	-	0.02	0.21
146	-CH ₂ -C ₆ H ₄ -I	CH ₃	OCH ₃	CO ₂ H	-	-	> 4	0.08
147	-CH ₂ -C ₆ H ₄ -Br	CH ₃	OCH ₃	CH ₂ NH ₂	-	-	> 4	0.67
148	H	CH ₃	OCH ₃	CO ₂ H	-	-	> 4	> 4
149	-SO ₂ NH ₂	CO ₂ H	-	-	-	-	> 4	> 4
150	-SO ₂ CH ₃	CO ₂ H	-	-	-	-	> 4	> 4
151	-SO ₂ NH ₂	-(CH ₂) ₂ CO ₂ H	-	-	-	-	> 25	8.90
152	-SO ₂ CH ₃	-(CH ₂) ₂ CO ₂ H	-	-	-	-	> 25	> 4
-	Indomethacin	-	-	-	-	-	0.05	0.75
-	Celecoxib	-	-	-	-	-	> 4	0.03
-	Ketoprofen	-	-	-	-	-	0.05	0.72
-	Flurbiprofen	-	-	-	-	-	0.16	0.09

^aIC₅₀ values were determined as described in Experimental Procedures. Assays were run in duplicate.

So, COX-2 expression in the 1483 tumor seems to be required for this selective uptake, although other factors besides the level of COX-2 protein may contribute to the relative enrichment over the control tissues. This result supports the hypothesis that the difference in labeling of 1483 and HCT116 xenografts is due to their differential in COX-2 expression, and confirms those reported previously for compound **41**.²⁷

DISCUSSION

The present report describes our SAR studies of fluorescent derivatives of NSAIDs or COXIBs as COX-2-selective inhibitors. The compounds were prepared using a conjugate-based strategy.²⁷ Some, but not all, fluorescent derivatives of NSAIDs or COXIBs, such as indomethacin or celecoxib, exhibit the ability to inhibit COX-2 selectively. This is consistent with our observation that nonselective carboxylic acid-containing NSAIDs can be transformed into COXIBs by converting them into amide or ester derivatives.³⁰ Relatively large fluorophore

moieties containing an alkyl, aryl, aralkyl, polyethylene glycol, or heterocyclic esters or amides of indomethacin or celecoxib exhibit COX-2 inhibitory activity. It is noteworthy that, among the fluorescent conjugates of NSAIDs or COXIBs that were evaluated in this study, only indomethacin derivatives bind tightly to COX-2 without binding to COX-1. Therefore, tethering fluorescent tags at the carboxylic acid site of indomethacin generates optical probes that are potent and selective COX-2 inhibitors.

The COX active site is located at the top of a deep channel that runs from the membrane-binding domain into the catalytic domain.³¹ The initial portion of the channel has a large volume, termed the lobby, which narrows at the top into a constriction comprising residues Arg-120, Tyr-355, and Glu-524.³² These residues must open and close in order for substrates and inhibitors to pass into or out of the COX active site, which is located above it. The use of the long alkyl, aryl, phenylene, polyethylene glycol, or heterocyclic chain allows the

Table 7. In Vitro Cell Line Assay Data of Promising Compounds

No	RAW264.7 IC ₅₀ (μM) ^a	1483 HNSCC IC ₅₀ (μM) ^b
1	0.10	NT
13	0.02	NT
14	0.04	NT
15	0.06	NT
16	0.18	NT
20	0.57	NT
23	> 5	NT
33	> 5	NT
36	2.00	NT
38	> 5	NT
41	0.31	0.09
49	0.36	NT
51	1.60	NT
58	0.34	0.38
65	0.08	NT
79	8.90	NT
125	0.50	NT

^aIC₅₀ values were determined as described in Experimental Procedures for RAW264.7 macrophage-like cells. ^bIC₅₀ values were determined as described in Experimental Procedures for human head and neck squamous cell carcinoma (HNSCC), 1483 cells. The NT designation indicates that cell line assay results were not tested.

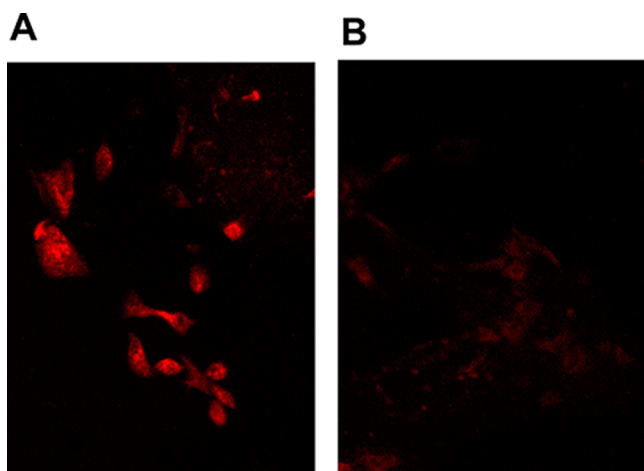


Figure 2. Labeling of COX-2-expressing cells by compound 58. The experimental protocols are described in Experimental Procedures. (A) 1483 HNSCC cells treated with 200 nM compound 58 for 30 min. (B) 1483 HNSCC cells pretreated with 5 μM indomethacin for 20 min prior to compound 58 treatment.

indomethacin functionality to fully insert into the binding pocket of COX-2, while the bulky fluorescent secondary amide functional group projects through the constriction at the base of the active site and into the wide lobby in the membrane-binding domain. This model, which is consistent with the crystal structure of a complex of COX-2 with a carboxyl chain-extended analogue of zomepirac,³³ helps to explain how such large moieties as 5- and 6-ROX can be conjugated to indomethacin with retention of inhibitory activity.

The systematic evaluation of a large number of conjugates generated from a wide variety of carboxylic acid-containing core molecules, tethers, and fluorophores provides some key insights into the structural requirements for COX-2-selective inhibition. For example, the results showed that as the number of methylene groups in the alkyl linker increased from 2 to 4, the inhibitory activity of conjugates was increased in an ordered fashion. A further increase ($n = 5$ to $n = 14$) in methylene groups or incorporation of additional amide groups in the

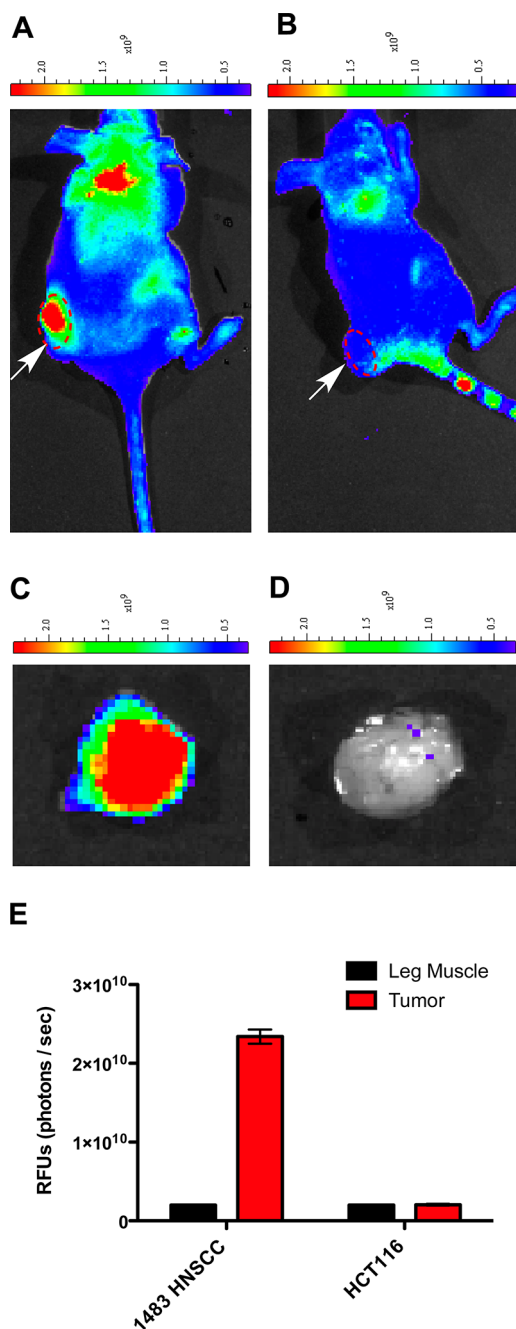


Figure 3. In vivo labeling of COX-2-expressing xenografts by compound 58. (A) Nude mice with 1483 xenograft (COX-2 positive) or HCT116 xenograft (B, COX-2 negative) on the left flank were dosed intraperitoneally with compound 58 (2 mg/kg) and imaged at 3 h postinjection. (C) Ex vivo fluorescence image of 1483 xenograft tumor at 4.5 h postinjection of 58. (D) Ex vivo fluorescence image of HCT116 xenograft tumor at 4.5 h postinjection of 58, showing a significant tumor uptake difference between COX-2 positive versus COX-2 negative tumor models. (E) Software measurement of light emission from the 1483 versus HCT116 xenograft tumor at 4.5 h postinjection of 58, as compared with leg muscle ($n = 4$). RFU, relative fluorescence units.

tether reversed the trend of inhibitory activity, suggesting that an *n*-butyl linker was optimal for selective COX-2 inhibition by these conjugates. In addition, the activity varied depending on the number of amide-linkages in the chain. However, hybrid linkers (i.e., alkyl and PEG or alkyl and piperazine) were

tolerated to some extent. The activity of conjugates also depended on the size and electronic properties of the fluorophores. Fluorophores having molecular weight of <650 without a charged atom afforded effective COX-2 inhibitory potencies. For example, coumarin or dansyl fluorophores are uncharged and have a molecular weight of <650. Indomethacin-coumarinylamide (**5**) was a highly potent and selective COX-2 inhibitor, and as the coumarin fluorophore was replaced by an uncharged dansyl fluorophore, the extent of COX-2 selectivity and potency of the conjugate (**15**) remained unchanged. In contrast, fluorophores with a favorable molecular weight but containing a charged atom that ion-pairs with an external oppositely charged ion afforded indomethacin conjugates (e.g., **74–78**) that did not inhibit COX isozymes. Furthermore, conjugating the polar IRDye800 trisodium salt or polycarboxylic lanthanide chelators with indomethacin yielded inactive compounds (**85–106**). Interestingly, zwitterionic fluorophores, such as 5- or 6-ROX, conjugated with indomethacin through an *n*-butyl linker afforded selective and potent COX-2 inhibitors (e.g., **41** and **49**). ROX fluorophores proved to be the optimal functional groups for effective COX-2 binding of their conjugates. Although indomethacin conjugates of dansyl, dabsyl, coumarin, or related fluorophores exhibited promising COX-2 inhibition in purified protein and in intact cells, they did not possess fluorescence properties suitable for in vivo imaging.

Among the compounds that emerged from our development pathway, only the 5-ROX- and 6-ROX-based conjugates (linker = *n*-Butyl) exhibited the necessary combination of adequate photophysical properties and effective COX-2 inhibitory potencies. As we previously reported,²⁷ the 5-ROX and 6-ROX conjugates (compounds **41** and **49**) show great promise as in vivo imaging agents for inflammation and cancer. Here, we have expanded those findings, through the demonstration that compound **58** also displays a very high degree of selectivity of uptake by intact cells in tissue culture and tumors in live animals. The selective delivery of compound **58** requires the expression of COX-2 at the target site and is not seen when COX-2 is not expressed. Thus, these fluorocoxibs are capable of targeting COX-2 in intact cells and tumors that express COX-2 in both in vitro and in vivo settings. Thus, conversion of NSAIDs or COXIBs into their fluorescent derivatives provides a facile strategy for generating effective imaging agents for detection of COX-2 in premalignant and malignant tumors. Also, this facile strategy provides proof-of-principle for the development of COX-2-specific NSAID or COXIB–toxin conjugates (Chemocoxibs) enabling selective delivery of cytotoxic agents into neoplastic cells for the treatment of premalignant and malignant tumors.

CONCLUSIONS

We describe the SAR of a series of optical imaging agents comprising bulky fluorescent functional groups tethered onto NSAIDs or COXIBs to create dual function fluorescent COX-2 inhibitors. A wide variety of fluorescent conjugates were synthesized and evaluated as COX-2-selective inhibitors against both purified protein and COX-2-expressing human cancer cells. The SAR study revealed that indomethacin conjugates afford the best COX-2 inhibitors compared to conjugates of other carboxylic acid-containing NSAIDs or COXIBs. A four-carbon *n*-alkyl linker is optimal for conjugating bulky zwitterionic fluorescent functionalities, such as ROX, to provide the best balance between selectivity and potency of COX-2 binding. Fluorophores that are metal or halide salts, such as IRDye800 or

NIR667, or organic polycarboxylic acid-containing functional groups that are highly polar, such as lanthanide chelators, are not suitable for developing COX-2-targeted imaging agents.

ASSOCIATED CONTENT

Supporting Information

Full synthetic procedures and analytical and spectral characterization data of synthesized compounds. This material is available free of charge via the Internet at <http://pubs.acs.org>.

AUTHOR INFORMATION

Corresponding Author

*Phone: 615-343-7329. Fax: 615-343-7534. E-mail: larry.marnett@vanderbilt.edu.

Notes

The authors declare the following competing financial interest(s): Drs. Uddin, Crews, and Marnett are inventors on a patent that describes the synthesis of COX-2-targeted imaging agents. The patent has been licensed and compounds are being marketed for use in preclinical experiments.

ACKNOWLEDGMENTS

This work was supported by research grants from the National Institutes of Health (CA136465, CA128323, CA89450). We are grateful to H. Charles Manning for assistance with lanthanide chelator synthesis and Carol Rouzer for critical reading and editing of this manuscript.

ABBREVIATIONS

COX, cyclooxygenase; SAR, structure–activity relationship; NSAID, nonsteroidal anti-inflammatory drug; COXIB, COX-2-selective inhibitor; DMEM, Dulbecco's Modified Eagle Medium; HNSCC, head and neck squamous cell carcinoma; BOC, *tert*-butoxycarbonyl; PEG, polyethylene glycol; NIR, near-infrared; DOTA, 1,4,7,10-tetraazacyclododecane-1,4,7,10-tetraacetic acid; ROX, carboxy-X-rhodamine

REFERENCES

- (1) Licha, K.; Riefke, B.; Ntziachristos, V.; Becker, A.; Chance, B., and Semmler, W. (2000) Hydrophilic cyanine dyes as contrast agents for near-infrared tumor imaging: synthesis, photophysical properties and spectroscopic in vivo characterization. *Photochem. Photobiol.* 72, 392–398.
- (2) Becker, A.; Riefke, B.; Ebert, B.; Sukowski, U.; Rinneberg, H.; Semmler, W., and Licha, K. (2000) Macromolecular contrast agents for optical imaging of tumors: comparison of indotricarbocyanine-labeled human serum albumin and transferrin. *Photochem. Photobiol.* 72, 234–241.
- (3) Neri, D.; Carnemolla, B.; Nissim, A.; Leprini, A.; Querzè, G.; Balza, E.; Pini, A.; Tarli, L.; Halin, C.; Neri, P.; Zardi, L., and Winter, G. (1997) Targeting by affinity-matured recombinant antibody fragments of an angiogenesis-associated fibronectin isoform. *Nat. Biotechnol.* 15, 1271–1275.
- (4) Ntziachristos, V.; Tung, C.-H.; Bremer, C., and Weissleder, R. (2002) Fluorescence molecular tomography resolves protease activity in vivo. *Nat. Med.* 8, 757–760.
- (5) Blum, G.; Mullins, S. R.; Keren, K.; Fonovic, M.; Jedszko, C.; Rice, M. J.; Slone, B. F., and Bogoy, M. (2005) Dynamic imaging of protease activity with fluorescently quenched activity-based probes. *Nat. Chem. Biol.* 1, 203–209.
- (6) Achilefu, S.; Bloch, S.; Markiewicz, M. A.; Zhong, T.; Ye, Y.; Dorshow, R. B.; Chance, B., and Liang, K. (2005) Synergistic effects of light-emitting probes and peptides for targeting and monitoring integrin expression. *Proc. Natl. Acad. Sci. U.S.A.* 102, 7976–7981.

- (7) Folli, S., Westermann, P., Braichotte, D., Pèlegri, A., Wagnières, G., van den Bergh, H., and Mach, J. P. (1994) Antibody-indocyanineconjugates for immunophotodetection of human squamous cell carcinoma in nude mice. *Cancer Res.* 54, 2643–2649.
- (8) Ballou, B., Fisher, G. W., Waggoner, A. S., Farkas, D. L., Reiland, J. M., Jaffe, R., Mujumdar, R. B., Mujumdar, S. R., and Hakala, T. R. (1995) Tumor labeling in vivo using cyanine-conjugated monoclonal antibodies. *Cancer Immunol. Immunother.* 41, 257–263.
- (9) Weissleder, R., Tung, C.-H., Mahmood, U., and Bogdanov, A., Jr. (1999) In vivo imaging of tumors with protease-activated near-infrared fluorescent probes. *Nat. Biotechnol.* 17, 375–378.
- (10) Tung, C.-H., Lin, Y., Moon, W. K., and Weissleder, R. (2002) A receptor-targeted near-infrared fluorescence probe for in vivo tumor imaging. *ChemBioChem* 8, 784–786.
- (11) Chen, X., Sievers, E., Hou, Y., Tohme, M., Bart, R., Bremner, R., Bading, J. R., and Conti, P. S. (2005) Integrin $\alpha_v\beta_3$ -targeted imaging of lung cancer. *Neoplasia* 7, 271–279.
- (12) Vane, J. R. (1971) Inhibition of prostaglandin synthesis as a mechanism of action for aspirin-like drugs. *Nat. New Biol.* 231, 232–235.
- (13) Smith, W. L., Garavito, R. M., and DeWitt, D. L. (1996) Prostaglandin endoperoxide H synthases (cyclooxygenases)-1 and -2. *J. Biol. Chem.* 271, 33157–33160.
- (14) Li, G., Yang, T., and Yan, J. (2002) Cyclooxygenase-2 increased the angiogenic and metastatic potential of tumor cells. *Biochem. Biophys. Res. Commun.* 299, 886–890.
- (15) Taketo, M. M. (1998) Cyclooxygenase-2 inhibitors in tumorigenesis (part II). *J. Natl. Cancer Inst.* 90, 1609–1620.
- (16) Taketo, M. M. (1998) COX-2 and colon cancer. *Inflammation Res.* 47, 112–116.
- (17) Abdalla, S. I., Lao-Sirieix, P., Novelli, M. R., Lovat, L. B., Sanderson, I. R., and Fitzgerald, R. C. (2004) Astrin-induced cyclooxygenase-2 expression in Barrett's carcinogenesis. *Clin. Cancer Res.* 10, 4784–4792.
- (18) Sano, H., Kawahito, Y., Wilder, R. L., Hashiramoto, A., Mukai, S., Asai, K., Kimura, S., Kato, H., Kondo, M., and Hla, T. (1995) Expression of cyclooxygenase-1 and -2 in human colorectal cancer. *Cancer Res.* 55, 3785–3789.
- (19) Shirvani, V. N., Ouatu-Lascar, R., Kaur, B. S., Omary, M. B., and Triadafilopoulos, G. (2000) Cyclooxygenase 2 expression in Barrett's esophagus and adenocarcinoma: Ex vivo induction by bile salts and acid exposure. *Gastroenterology* 118, 487–496.
- (20) Gupta, R. A., and DuBois, N. (2002) Cyclooxygenase-2 inhibitor therapy for the prevention of esophageal adenocarcinoma in Barrett's esophagus. *J. Natl. Cancer Inst.* 94, 406–407.
- (21) Maier, T. J., Schilling, K., Schmidt, R., Geisslinger, G., and Grosch, S. (2004) Cyclooxygenase-2 (COX-2)-dependent and -independent anticarcinogenic effects of celecoxib in human colon carcinoma cells. *Biochem. Pharmacol.* 67, 1469–1474.
- (22) Vries, E. F. J. D., Waarde, A. V., Buursma, A. R., and Vaalburg, W. (2003) Synthesis and in vitro evaluation of ^{18}F -desbromo-DuP-697 as a PET tracer for cyclooxygenase-2 expression. *J. Nucl. Med.* 44, 1700–1706.
- (23) McCarthy, T. J., Sheriff, A. U., Graneto, M. J., Talley, J. J., and Welch, M. J. (2002) Radiosynthesis, in vitro validation, and in vivo evaluation of ^{18}F -labeled COX-1 and COX-2 inhibitors. *J. Nucl. Med.* 43, 117–124.
- (24) Schuller, H. M., Kabalka, G., Smith, G., Meredy, A., Akula, M., and Cekanova, M. (2006) Detection of overexpressed COX-2 in precancerous lesions of hamster pancreas and lungs by molecular imaging: implications for early diagnosis and prevention. *ChemMedChem* 1, 603–610.
- (25) Uddin, M. J., Crews, B. C., Ghebreselasie, K., Huda, I., Kingsley, P. J., Ansari, M. S., Tantawy, M. N., Reese, J., and Marnett, L. J. (2011) Fluorinated COX-2 inhibitors as agents in PET imaging of inflammation and cancer. *Cancer Prev. Res.* 7, 1536–1545.
- (26) Uddin, M. J., Crews, B. C., Ghebreselasie, K., Tantawy, M. N., and Marnett, L. J. (2010) [^{123}I]-Celecoxib analogs as SPECT tracer of cyclooxygenase-2 (COX-2) in inflammation. *ACS Med. Chem. Lett.* 2, 160–164.
- (27) Uddin, M. J., Crews, B. C., Blobaum, A. L., Kingsley, P. J., Gorden, D. L., McIntyre, J. O., Matrisian, L. M., Subbaramaiah, K., Dannenberg, A. J., Piston, D. W., and Marnett, L. J. (2010) Selective visualization of cyclooxygenase-2 in inflammation and cancer by targeted fluorescent imaging agents. *Cancer Res.* 70, 3618–3627.
- (28) Zweifel, B. S., Davis, T. W., Ornberg, R. L., and Masferrer, J. L. (2002) Direct evidence for a role of cyclooxygenase 2-derived prostaglandin E2 in human head and neck xenograft tumors. *Cancer Res.* 62, 6706–6711.
- (29) Sheng, H. M., Shao, J. Y., and Kirkland, S. C. (1997) Inhibition of human colon cancer cell growth by selective inhibition of cyclooxygenase-2. *J. Clin. Invest.* 99, 2254–2259.
- (30) Kalgutkar, A. S., Crews, B. C., Rowlinson, S. W., Marnett, A. B., Kozak, K. R., Rummel, R. P., and Marnett, L. J. (2000) Biochemically based design of cyclooxygenase-2 (COX-2) inhibitors: Facile conversion of nonsteroidal antiinflammatory drugs to potent and highly selective COX-2 inhibitors. *Proc. Natl. Acad. Sci. U.S.A.* 97, 925–930.
- (31) Kurumbail, R. G., Stevens, A. M., Gierse, J. K., McDonald, J. J., Stegeman, R. A., Pak, J. Y., Gildehaus, D., Miyashiro, J. M., Penning, T. D., Seibert, K. P., Isakson, C., and Stallings, W. C. (1996) Structural basis for selective inhibition of cyclooxygenase-2 by anti-inflammatory agents. *Nature* 384, 644–648.
- (32) Picot, D., Loll, P. J., and Garavito, R. M. (1994) The X-ray crystal structure of the membrane protein prostaglandin H₂ synthase-1. *Nature* 367, 243–249.
- (33) Luong, C., Miller, A., Barnett, J., Chow, J., Ramesha, C., and Browner, M. F. (1996) Flexibility of the NSAID binding site in the structure of human cyclooxygenase-2. *Nat. Struct. Biol.* 3, 927–933.